

Research Article

Stress Testing of Steel Suspender of Arch Bridge Model Based on Induced Magnetic Flux Method

Guangyuan Weng ¹, Liu Yang,² and Zhu Xiyu ¹

¹Mechanical Engineering College, Xi'an Shiyou University, Xi'an 710065, China

²School of Urban Planning and Municipal Engineering, Xi'an Polytechnic University, Xi'an 710048, China

Correspondence should be addressed to Guangyuan Weng; weng_guangyuan@163.com

Received 13 December 2019; Accepted 16 January 2020; Published 14 February 2020

Academic Editor: Guoqiang Xie

Copyright © 2020 Guangyuan Weng et al. This is an open access article distributed under the Creative Commons Attribution License, which permits unrestricted use, distribution, and reproduction in any medium, provided the original work is properly cited.

To establish an online nondestructive stress testing method for arch bridge suspender based on the principle of magnetic coupling, the magnetic mechanical property of Q345qD steel is explored taking an arch bridge model structure with Q345qD steel suspender as the research object. Under the action of magnetic field excited by a coil, the test of the coupling relationship between stress and excitation flux is carried out. The theoretical model of stress-magnetic flux is simplified to better meet the requirements of engineering applications. The excitation device, magnetic flux measurement device, stress-magnetic flux data analysis program, and so on are developed, and the magnetic coupling stress detection system is integrated. The test model structure of a steel arch bridge with suspenders of Q345qD alloy steel is designed and made; under the different load conditions, the stresses of the suspenders are tested and studied. The relationships between induced magnetic flux and technical magnetized voltage, test load of model structure, and different stress conditions of the suspenders are analyzed; with the induction magnetic flux as the parameter, the stress-magnetic flux coupling model is established. The test results based on the stress-magnetic flux coupling model are compared with those of the traditional stress-strain test in a linear elastic range; it shows that the two testing methods are in good agreement with each other, and the maximum error is less than 5%. Meanwhile, with the increase in the load on the suspender, the tension stress increases and the induced magnetic flux decreases, showing a good linear relationship. The conclusions drawn from the research can provide important reference for health monitoring of suspenders of arch bridges.

1. Introduction

The suspender of the long-span steel arch bridge is the key stress structural member. During the construction, operation, and maintenance, suspender is affected by the changes in load, material properties, and environment. The actual stress state during the service period is inconsistent with the design, even reaching or exceeding the design limitation, resulting in major engineering safety incidents in the application of steel bridge structures. The traditional testing techniques and methods are mainly based on the stress-strain constitutive model. It is necessary to consider the loading path and material nonlinearity of the load. In addition, the strain monitoring is not easy to realize for the structure of complex service environment. Therefore, it is difficult for traditional testing technology to detect the

real-time online tensile strength of suspenders of long-span steel arch bridges, and it is also difficult to monitor the changes in material properties of key parts of the suspender under stress. Stress detection theory based on the magnetic coupling effect is a new type of magnetic nondestructive testing method developed in recent years [1–12]. The basic principle is based on the magnetic coupling theory of ferromagnetic materials [13–15]. Under the action of external stress, the inverse magnetostrictive effect of ferromagnetic materials changes its internal magnetic energy [16–18]. The magnetic parametric-stress model for stress detection is established by using the relationship between the magnetic properties and the stress of the metal structural member [19–22]. This method does not need to consider the loading history and material nonlinearity and can overcome the shortcomings of traditional detection technology [23–25].

Scholars have carried out related research work on the theory and application of the magnetic coupling effect [26, 27].

2. Magnetic Properties

2.1. Bridge Structural Steel Magnetization Performance. According to the stress characteristics and service environment of the steel bridge structure, in the smelting process of common structural steels, the contents of C, Si, Mn, S, P, and other elements are often controlled. Among them, the content of C is the main factor affecting the magnetic properties. The C content has an important effect on the maximum permeability μ_{\max} and the coercive force H_c [28]; at the same time, it also hinders the movement of the magnetic domain structure and affects the magnetic coupling effect. This study is based on the components of common bridge structural steel and studies the stress detection based on the magnetic coupling effect. The weight percentage of pearlite is about 10%~20%, the weight percentage of ferrite is about 90%~75%, and the weight percentage of carbon content in steel is about 0.08%~0.20%.

Bridge structural steel, as one of the wide variety of magnetic materials, has similar magnetic properties, but the magnetic domain structure and its movement are different. Due to the different production process, composition, structure with other general ferromagnetic materials, the magnetization process, and magnetization performance, parameters of the bridge structural steel are also different mainly in the shape of the magnetization curve and the hysteresis curve. To find out the magnetization mechanism of common bridge structural steel, the magnetization curve of the specimen with the grade Q345qD and diameter of 32 mm is tested by the SQUID-VSM magnetic measurement system. In the test, by loading the magnetic field at a rate of 100 Oe/s at different temperatures, the corresponding relationship between the magnetic field strength and the magnetic moment is obtained, and then the B-H relationship curve is calculated. The Gaussian unit system is selected, the unit of the magnetic moment is emu, the unit of the magnetic field H is Oe (10,000 Oe is equivalent to 1 T), and the magnetization of the specimen is equal to the ratio of the magnetic moment to the volume. Figure 1 shows the initial magnetization curve of the Q345qD bridge structural steel specimen under normal temperature conditions from -1.0 T to 1.0 T.

It can be seen from Figure 1 that the magnetization curve of the bridge structural steel is substantially similar to the magnetization curve of the general ferromagnetic material. The shape of the magnetization curve is slender, which indicates that the bridge structure steel Q345qD has the characteristics of high permeability and low coercivity. Although impurities such as carbon, nitrogen, oxygen, and sulfur have influence on magnetic properties, the magnetic parameters tested in this study can meet the requirements of stress testing. When the magnetic saturation state is reached, the variation in the magnetic field strength is small after the magnetization is saturated. The maximum magnetization is $1.98 \text{ A}\cdot\text{m}^2$.

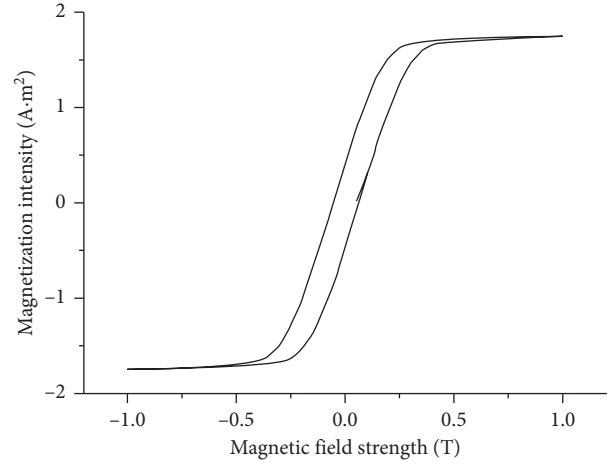


FIGURE 1: Magnetization curve of bridge steel Q345qD.

2.2. Stress-Magnetic Flux Coupling Model. As the stress changes, the magnetic domain structure of the bridge structure steel changes. As the magnetic field conditions change, the induced magnetic flux of the specimen changes. In this paper, in the elastic range under the action of active tension, the coupling relationship between the axial stress of the specimen and the induced magnetic flux is researched.

The bridge structural steel belongs to the polycrystalline ferromagnetic material. When the stress and the external excited magnetic field act simultaneously, the parametric which characterizes the magnetic property also changes. When the specimen is subjected to the axial stress, the axial deformation causes the magnetization to change. For ferromagnetic materials [29],

$$\sigma = \frac{3\lambda_s M_s E}{2K_u} B \sin^2 \theta_0 \cos \theta_0, \quad (1)$$

where σ is the stress of the specimen, λ_s is the axial deformation constant, M_s is the saturation magnetization, K_u is the uniaxial magnetic anisotropy constant, E is the elastic modulus of ferromagnetic materials, B is the magnetic flux density, and Φ is the angle between the magnetic field and the easy axis of magnetization. The formula (1) expresses the relationship between the stress and the induced magnetic flux of the ferromagnetic material sample under the action of magnetic field and establishes the theoretical model of the stress-induced magnetic flux of the general ferromagnetic material. It is an important theoretical basis for the stress test technology by the induced magnetic flux method. Bridge structural steel is a kind of ferromagnetic material, and its stress-induced magnetic flux constitutive relation accords with formula (1). However, when testing the stress of the structural member made of bridge structural steel, the parameters of formula (1) involve the microscopic mechanism of ferromagnetic materials, which is difficult to determine in practical engineering applications. For this reason, the test of stress-induced magnetic flux coupling relationship for the Q345qD bridge structural steel specimen is done, and a practical model of stress detection based on magnetic coupling theory is obtained. In the test, the magnetic field is

generated by the excitation coil that is adjusted by the adjustable power source, the induced magnetic flux of the specimen is measured by the TD8900 magnetic flux meter, and the specimen is loaded by the WAW-1000 micro-computer controlled electrohydraulic servo universal testing machine.

In the data processing of the tensile stress-induced magnetic flux constitutive model, only the main magnetic flux is considered, and the leakage magnetic flux is ignored. The distribution of flux at any cross section of the specimen in the magnetic circuit is uniform. When the specimen is loaded to yield, the coupling relationship between the stress and the induced magnetic flux is shown in Figure 2.

It can be seen from Figure 2 that when the tensile stress of the bridge structural steel specimen increases, the induced magnetic flux also increases, and the rate of increase is slightly lower than the rate of stress increase. In the state of technical magnetization saturation, the induced magnetic flux remains substantially unchanged when the specimen reaches the yield strength. Data fitting of the curve of Figure 2 is carried out to obtain the constitutive equation of the magnetic flux change value and tensile stress of the Q345qD bridge structural steel specimen:

$$\sigma = a - b \times \ln(\Delta\Phi),$$

$$\Delta\Phi = \frac{\Phi_2 - \Phi_1}{\Phi_1},$$

$$a = 28.860 + 0.832 \times f_{yk} - 7.921 \times d - 0.0074 \times f_{yk} \times d,$$

$$b = 0.896 - 0.325 \times f_{yk} + 0.0002 \times d,$$

(2)

where σ is the stress value, and the unit is MPa. $\Delta\Phi$ is the amount of change in magnetic flux; Φ_1 is the magnetic flux corresponding to the stress of the specimen during the previous loading step during loading; and Φ_2 is the magnetic flux corresponding to the stress of the specimen during the next loading step during loading, and their unit is mWb. a and b are the parameter determined by the diameter of the grade and the round steel. f_{yk} is the standard value of the yield strength of the bridge structure steel, and the unit is MPa. d is the diameter of the test specimen, and the unit is mm. When $\sigma \leq 300$ MPa, the stress-induced magnetic flux model of Q345qD bridge structural steel can be simplified by the curve in Figure 2 and fitting formula (2), which can better meet the needs of stress testing.

3. Magnetic Coupling Stress Testing System

3.1. Excitation System. According to the structural characteristics of the arch bridge model structure, the hollow coil sleeve type excitation device system is designed. The probe uses a field coil to generate a magnetic field to magnetize the member to be tested. The magnetic field generated by the field coil has a great influence on the structural design and measurement effect of the probe. Therefore, it is necessary to study the formation mode and distribution of the magnetic

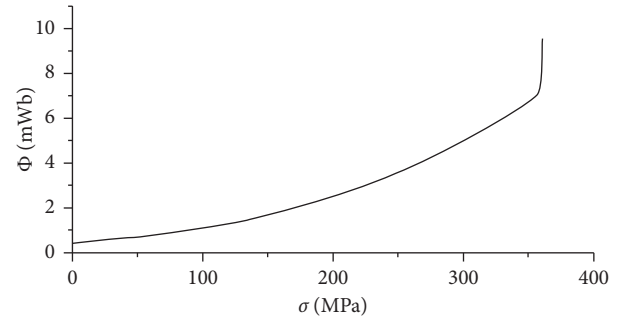


FIGURE 2: Curve of stress-induced flux coupling.

field in the exciting coil. A reasonably designed excitation coil is required to have a strong technology property and to form a nearly uniform magnetic field inside the coil in which the member to be tested is contained. After repeated trial calculations and magnetic characteristics test, two kinds of excitation coils for the stress detection of different diameter suspenders in the test model structure are developed. The performance parameters are shown in Table 1.

To achieve the desired magnetization state of the stress sensitive area of the suspenders to be tested, it is usually necessary to provide a sufficiently large magnetic field excited by an adjustable DC power source. First, calculate the working magnetic field by calculating the axial centre magnetic field of the coil (at the maximum position of the magnetic field) and estimate the voltage of the required DC power supply. In the actual test and control, the basic principle of capacitor charging and discharging is used to generate enough adjustment.

3.2. Magnetic Induction Measuring Device System. The magnetic induction coil is used to measure the magnetic flux passing through the cross section of the test specimen, and the measuring coil circuit generates a constant magnetic field in the closed loop formed by the probe and the sample to be tested. The measuring coil is made of 0.3 mm enameled wire and wound 150–300 turns. The magnetic flux measurement performance of the magnetic induction coil is tested by using 300–400 mA DC current. According to the test results, two different types of measuring coils were developed. The measuring coil is connected to the TD8900 flux meter to measure the change in magnetic flux through the cross section of the specimen. The relevant content of the measuring coil is similar to that of the magnetic field excitation coil, which will not be discussed here.

The excitation device, the magnetic induction measuring device, and the measured data processing program are integrated to form a magnetic coupling stress detecting system. In this study, the stress and strain tests are also carried out while designing and testing the magnetic coupling system. Before the test, a strain sensor is placed on each member, and when loaded, the stress of each member is obtained based on the measured strain. The results obtained by the linear elastic stress-strain test system is used as the control group of the magnetic coupling test results to test the validity of the

TABLE 1: Technical parameters of the exciting coil.

Coil name	Length-diameter ratios	Turns	Conductor diameter (mm)	Coil inner diameter (mm)
JLXQ-1	10	2000	0.2	12
JLXQ-2	10	1000	0.2	6

results. The stress-strain test system adopts the traditional design method, which will not be repeated here.

4. Experimental Research and Result Analysis

4.1. Structural Design of Steel Arch Bridge Model. This experimental study designed a steel arch bridge structure model, as shown in Figure 3. The model structure is designed according to a project prototype using a 1:100 scale. The calculated span of the model structure is 1240 mm, the calculated height is 248 mm, and the height-span ratio is 1/4. The arch rib curve of the model structure is designed as a catenary, the cross section of the arch rib is a hollow circular cross section with an outer diameter D as 50 mm, and a horizontal connection is set between the two arch rings. In engineering practice, the suspender is usually made of steel strand; in this experiment, the main purpose is to make use of the magnetic coupling stress test system for the stress test and verify the validity of its application; therefore, the suspender in this arch model structure is made of Q345qD round steel. The length of the suspender can be adjusted by bolts at both ends to ensure that the position between the arch rib and the bridge floor is reasonable; at the same time, different diameter suspenders can be installed according to different test conditions. The bridge floor is designed as a steel truss beam and laid with steel plates. According to the principle of stiffness equivalent, for the convenience of production, the arch of the model structure is welded by a steel plate. According to this design, the steel bridge model structure can not only meet the test requirements of magnetic coupling stress testing but also has certain engineering application value.

4.2. The Model Structure Making. The arch rib adopts the representative steel grade SUS304 of the nonmagnetic iron system. The arch ring and the suspenders are bolted together, and the chord of the suspenders and bridge deck truss beam is also adopted through bolt connection. During the test, the suspenders can be exchanged to facilitate the stress test of different diameters or materials of the suspenders, and the connecting rod between the two arch ribs is welded. The model structure of the steel arch bridge is shown in Figure 4. In order to facilitate the analysis of the test results, the positions of the 16 suspenders of the model structure are numbered, as shown in Figure 4.

4.3. Loading Scheme. In the test, a concentrated load is applied to a steel plate supported by four force-transmitting steel short columns, and the load is evenly transmitted to the bridge deck by four force-transmitting steel short columns at equal points of the bridge deck length. It is loaded within the linear elastic range of the suspension in steps of 5 kN, and the

loading speed is controlled at 0.15–0.25 N/(mm²·s). The load in this test is a static load, and the applied load is shown in Figure 5. The curtain in Figure 5 is to reduce the interference of the environmental magnetic field in the test.

4.4. Test Results and Analysis. The magnetic coupling stress testing system developed by this study is used to carry out stress testing on the suspenders of the arch bridge model structure. Limited by the length of the paper, according to the symmetry of the model structure, from the test results of all tested suspenders, the test results of representative suspenders are only selected for analysis in detail, and the analysis method of the test results of other suspenders is the same. Taking the results of the stress testing of the model structure of the Q345 suspender with a diameter of 12 mm as an example, by analyzing the characteristics of changes in the excitation magnetic field parameters, magnetic induction parameters, stress, and strain, the relationship between magnetic and stress is revealed, and the corresponding application model of stress testing theory is proposed.

Figure 2 of this paper expresses the stress-induced magnetic flux curve of the Q345qD bridge structural steel, which can describe the relationship between the stress before the yield and the induced magnetic flux of the Q345qD bridge structural steel. The purpose of this test is to obtain a method for detecting the stress of the structural members of the arch bridge model by the magnetic coupling stress detection system and to analyze the effect of the test. Such a research purpose does not require stress of the suspender to reach 345 MPa. Therefore, in order to facilitate the experimental loading of the model structure, the loading stress of the suspender of the arch bridge model is controlled to 150 MPa, which can not only simplify the test but also achieve the purpose of the test.

4.4.1. Test Results of Suspender in Position 1. Under the excitation of the DC power supply, the excitation device magnetizes the suspension rod, and the magnetic induction measuring device is used to monitor the change of the magnetic flux of the model structure suspender under different excitation voltages. Figure 6 shows the stress-magnetic flux relationship of the suspender in position 1 when the input DC power supply voltage of the excitation device is 4 V, 6 V, 8 V, and 10 V, respectively.

It can be seen from Figure 6 that, after magnetization, under the action of constant excitation magnetic field strength, as the stress of the suspenders increases, the magnetic flux also becomes larger, and there is a substantially linear relationship. Under the same stress, the induced magnetic flux increases as the excitation voltage increases. In order to determine the optimal excitation voltage for stress testing, the relationship between the DC voltage and the

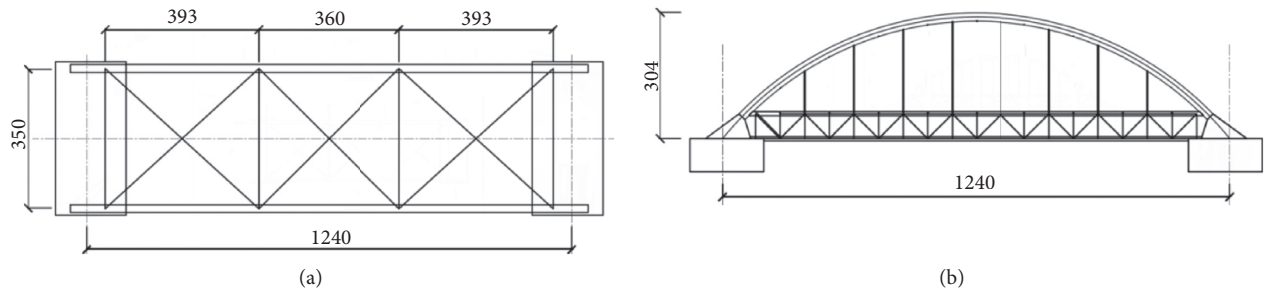


FIGURE 3: Model structure of steel arch bridge: (a) plan view of the steel arch bridge model (1 : 100); (b) elevation view of the steel arch bridge model (1 : 100).

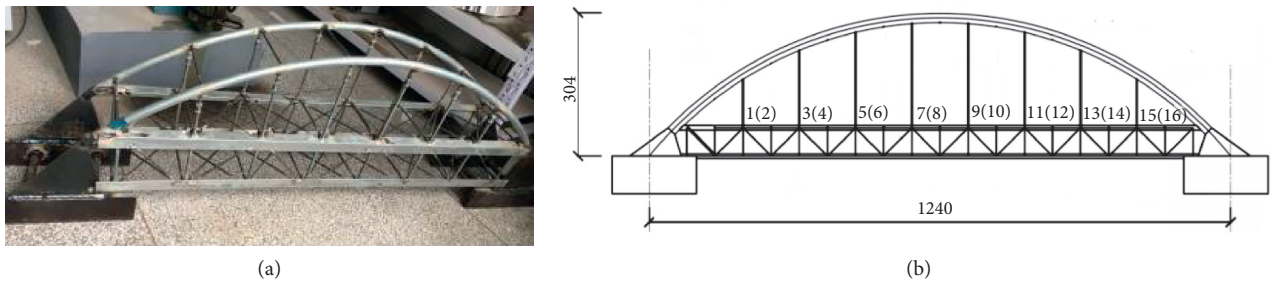


FIGURE 4: Picture of steel arch bridge model structures.

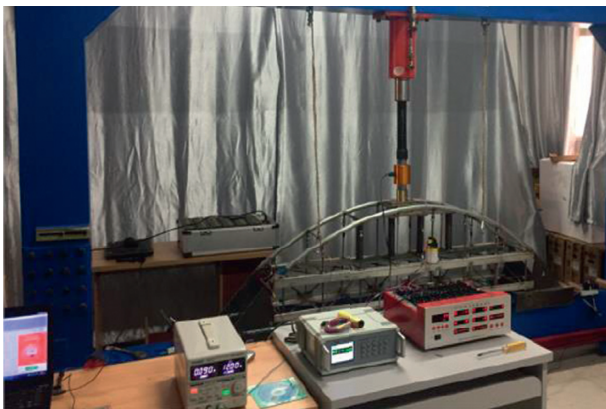


FIGURE 5: Model structure loading.

magnetic flux required for the excitation field strength of the excitation coil in the developed excitation device is studied, and the stress of the suspender at the 1st position is kept constant; when the excitation power supply voltage is 2 V, 4 V, 6 V, 8 V, 10 V, 12 V, and 14 V, the induced magnetic flux of the No. 1 position suspender is tested under different excitation voltage conditions, and the test result is shown in Figure 7.

As can be seen from Figure 7, the DC power supply voltage input to the excitation coil has an influence on the magnetic flux of the test suspender. When the excitation voltage does not exceed 10 V, the excitation voltage and magnetic flux basically have a linear relationship, and the

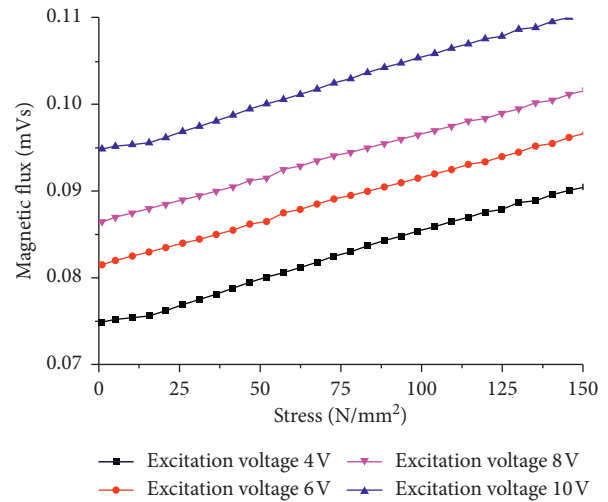


FIGURE 6: The relationships between stress and magnetic flux of No. 1 hanger rod.

induced magnetic flux increases with the excitation voltage at a faster rate. When it exceeds 10 V, the rate of the induced magnetic flux decreases with the increase in the voltage, basically does not increase, and maintains a relatively stable value, which indicates that the number 1 suspender is in a state of technical magnetization saturation when the excitation voltage is about 10 V.

In addition, Figure 7 also reflects the influence of the change of magnetic flux when different stress values. Under

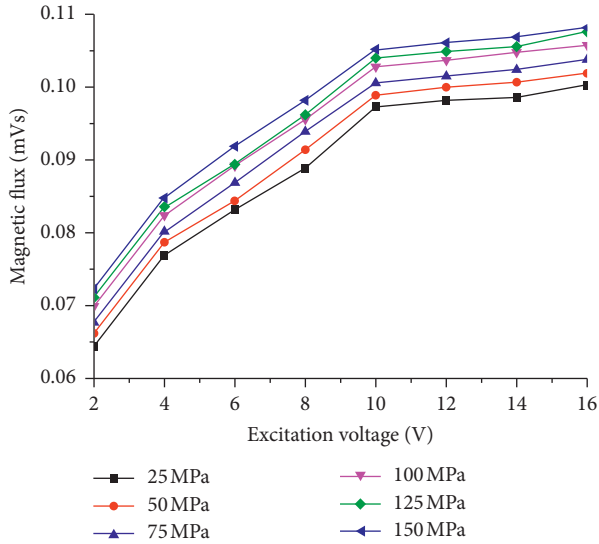


FIGURE 7: Relationships between the excitation voltage and magnetic flux of No. 1 position suspender.

the same excitation voltage condition, although the magnetic field strength of the technical magnetization is constant, the cross-sectional area of the suspenders decreases as the stress increases. The induced magnetic flux increases, and the tendency to increase with stress is basically the same. In addition, Figure 7 also reflects the effect of changes in magnetic flux at different stress values. Under the same excitation voltage condition, although the magnetic field strength of the technical magnetization is unchanged, as the stress increases, the cross-sectional area of the suspender decreases, so the measured induced magnetic flux increases, and the increasing tendency is basically the same as the increasing tendency with stress.

4.4.2. Induced Magnetic Flux of Suspender at Different Positions. In the study, the variation in the induced magnetic flux of the suspender at different positions under the same condition is further studied. According to the symmetry of the model structure, a quarter symmetrical structure is taken; that is, the suspension rods at positions 1, 3, 5, and 7 are taken as test objects; when the excitation voltage is 10 V, the induced magnetic flux of these suspension rods under different loads is shown in Figure 8.

It can be seen from Figure 8 that, under the same load, the inductive magnetic flux of the suspender with larger stress is also larger. When the magnetic field excitation is the same, under the action of tensile stress, the induced magnetic flux of the suspender at different locations increases with the increase in tensile stress, and the induced magnetic flux of the suspender at position 7 is the largest. From the perspective of bridge structure statics, combined with the loading of this test, the stress of the suspender at position 7 is the largest. This conclusion is consistent with the curve in Figure 8.

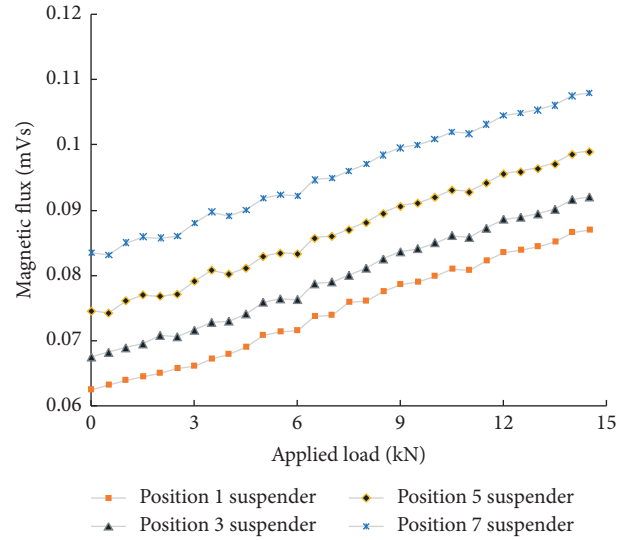


FIGURE 8: Induced magnetic flux at different hanger rod positions under the same load.

4.4.3. Comparison between Magnetic Stress Testing Method and Strain Test Results. In the magnetic stress testing of suspender, all the suspenders are within the linear elastic range; therefore, the stress-strain relationship in the model structure loading can be used to verify the validity of the magnetic coupling relationship. Firstly, the strain of the suspenders is measured by a strain gauge installed on the suspender, and the actual stress value of the suspender is obtained according to the stress-strain constitutive relationship of Q345qD. Secondly, according to the stress-magnetic flux relationship of Q345qD established in the foregoing, the induced magnetic flux is calculated. Finally, the induced magnetic flux under the same stress condition is measured and compared with the results obtained by the established stress-magnetic flux model to verify the validity of the stress-magnetic flux relationship of the arch bridge model structure. This paper gives the stress-magnetic flux linear regression equation of the No. 7 position suspender at the technical magnetization voltage of 10 V:

$$\Phi = 0.000082\sigma + 0.0628, \quad (3)$$

where Φ is the magnetic flux, σ is the stress derived from the relationship between stress and strain, and strain is the test value.

According to formula (3), the magnetic flux of suspender at position 7 under different stress conditions can be obtained, and the stress is obtained from the constitutive relation through the measured strain. By comparing the magnetic flux calculated by formula (3) with the magnetic flux measured in this paper, the error curve is shown in Figure 9.

It can be seen from Figure 9 that, under the same stress condition, compared by magnetic flux obtained by the stress-strain constitutive relation and the regression equation, the error of the magnetic flux detected by the developed

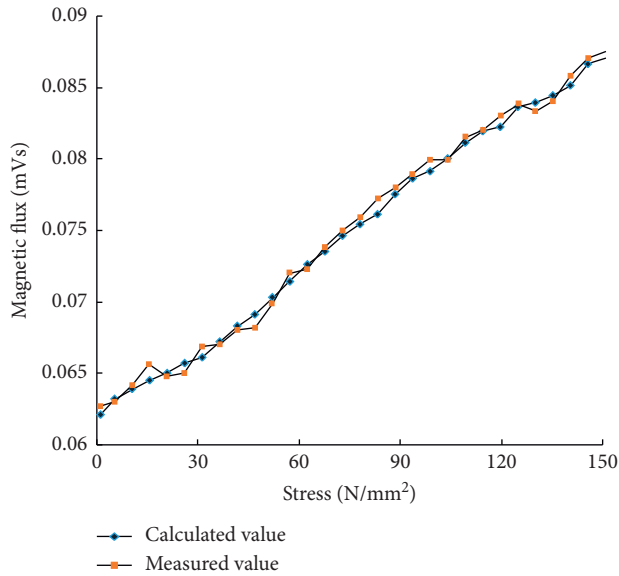


FIGURE 9: Error curves of calculated magnetic flux and measured value under the same stress condition.

magnetic coupling detection system are within 5%, which is very consistent and can meet the requirements of engineering applications.

5. Conclusion

Through the magnetic coupling stress testing of suspender of the steel arch bridge model structure, the main conclusions are as follows:

- (1) Under the action of external magnetic field, the induced magnetic flux of the bridge structural steel specimen with the grade Q345qD is related to the stress of the specimen. When $\sigma \leq 300$ MPa, the induced magnetic flux increases with the increase in stress, which is similar to the linear relationship.
- (2) The induced magnetic flux of the arch bridge model structure suspender are related to the stress of the suspender. When the technical magnetization reaches saturation, the induced magnetic flux and stress are basically linear.
- (3) Under the same magnitude loading condition of the arch bridge model structure, the induced magnetic flux of the suspender at different locations increases with the increase in the excitation voltage. The technical magnetization saturation excitation voltage of a suspender with a diameter of 12 mm is 10 V. Under the condition of technical magnetization saturation, the change trend of the induced magnetic flux of each suspender is basically the same.
- (4) In the range of linear elasticity, the stress obtained from the stress-strain constitutive relationship agrees well with the stress obtained from the magnetic coupling stress detection system developed in this study.

Data Availability

All data generated or analyzed during this study are included within the article.

Conflicts of Interest

The authors declare that they have no conflicts of interest.

Acknowledgments

This work was supported by the Key Research Development Program of Shaanxi (Program no. 2019SF-266), Project "Study on seismic fortification standards and damping method of gates and opening and closing facilities under the action of earthquake-Flow coupling (Grant nos. 2019JLM-54)" supported by Joint Foundation of Shaanxi, National Natural Science Foundation of China (51808446), and Shaanxi Natural Science Foundation (Grant no. 2018JQ5203).

References

- [1] Z. Qiu, W. Zhang, and Y. Guo, "Analysis of stress-magnetic coupling effect in weak magnetic environment," *Journal of Beijing Institute of Technology (English Edition)*, vol. 24, no. 4, pp. 471–477, 2015.
- [2] M. Föhnle and M. Komelj, "Nonlinear magnetoelastic coupling coefficients from simultaneous measurements of magnetostrictive stress and anisotropy in epitaxial magnetic films," *Journal of Magnetism and Magnetic Materials*, vol. 220, no. 1, pp. 13–17, 2000.
- [3] G. Wang, P. Yan, L. Wei, and Z. Deng, "The magnetic memory effect of ferromagnetic materials in the process of stress-magnetism coupling," *Advances in Materials Science and Engineering*, vol. 2017, Article ID 1284560, 8 pages, 2017.
- [4] G. Weng, Y. Shi, Y. Zhang, and J. Dai, "Application research on magnetic coupling stress testing technique for in-service steel bridge," *IOP Conference Series: Materials Science and Engineering*, vol. 649, no. 1, Article ID 012030, 2019.
- [5] Y. Xiao, H.-M. Zhou, and X.-L. Cui, "Nonlinear resonant magnetoelectric coupling effect with thermal, stress and magnetic loadings in laminated composites," *Composite Structures*, vol. 128, pp. 35–41, 2015.
- [6] G. Wang, L. Yang, and B. Liu, "Study on the testing method of oil-gas pipeline stress damage based on magnetic memory," *Yi Qi Yi Biao Xue Bao/Chinese Journal of Scientific Instrument*, vol. 38, no. 2, pp. 271–278, 2017.
- [7] S. Ren, Y. Ou, Z. Ren, and W. Yue, "Studies on stress-magnetism coupling effect for 35 steel components," *Insight-Non-Destructive Testing and Condition Monitoring*, vol. 52, no. 6, pp. 305–309, 2010.
- [8] C. Y. Tsai, H. R. Chen, F. C. Chang et al., "Stress-mediated magnetic anisotropy and magnetoelastic coupling in epitaxial multiferroic $\text{PbTiO}_3\text{-CoFe}_2\text{O}_4$ nanostructures," *Applied Physics Letters*, vol. 102, no. 13, Article ID 489760, 2013.
- [9] L. Bian, Y. Wen, Y. Wu et al., "A resonant magnetic field sensor with high quality factor based on quartz crystal resonator and magnetostrictive stress coupling," *IEEE Transactions on Electron Devices*, vol. 65, no. 6, pp. 2585–2591, 2018.
- [10] M. J. Dapino, R. C. Smith, L. E. Faidley, and A. B. Flatau, "A coupled structural-magnetic strain and stress model for

- magnetostrictive transducers,” *Journal of Intelligent Materials Systems and Structures*, vol. 11, no. 2, pp. 135–152, 2000.
- [11] L. Mierczak, D. C. Jiles, and G. Fantoni, “A new method for evaluation of mechanical stress using the reciprocal amplitude of magnetic Barkhausen noise,” *IEEE Transactions on Magnetics*, vol. 47, no. 2, pp. 459–465, 2011.
- [12] L. Mierczak, Y. Melikhov, and D. C. Jiles, “Residual Stress depth profiling using magnetic Barkhausen noise method,” in *Proceedings of the 50th Annual Conference of the British Institute of Non-Destructive Testing*, p. 257, Telford, UK, 2011.
- [13] M. Blaow, J. T. Evans, and B. Shaw, “Effect of deformation in bending on magnetic Barkhausen noise in low alloy steel,” *Materials Science and Engineering A*, vol. 386, no. 1-2, pp. 74–80, 2004.
- [14] J. Capó Sánchez, M. F. De Campos, and L. R. Padovese, “Magnetic Barkhausen emission in lightly deformed AISI 1070 steel,” *Journal of Magnetism and Magnetic Materials*, vol. 324, no. 1, pp. 11–14, 2012.
- [15] S. Sagar, N. Parida, S. Das, G. Dobmann, and D. Bhattacharya, “Magnetic Barkhausen emission to evaluate fatigue damage in a low carbon structural steel,” *International Journal of Fatigue*, vol. 27, no. 3, pp. 317–322, 2005.
- [16] L. Yang, H. Sun, and S. Gao, “The stress detection technology of steel plate based on coercivity,” *Non-Destructive Testing*, vol. 40, no. 3, pp. 5–9, 2018.
- [17] Z. Cheng, K. Song, and S. Dong, “Optimization and experimental study of stress detection based on MBN method,” *Non-Destructive Testing*, vol. 40, no. 4, pp. 13–18, 2018.
- [18] Z. Sun and J. Leng, “Design and fabrication of an electromagnetic stress sensor,” *Applied Mechanics and Materials*, vol. 128-129, pp. 567–570, 2012.
- [19] E.-G. Xiong, S.-L. Wang, and X.-Y. Miao, “Research on magnetomechanical coupling effect of Q235 steel member specimens,” *Journal of Shanghai Jiaotong University (Science)*, vol. 17, no. 5, pp. 605–612, 2012.
- [20] X. Min, L. Yang, G. Wang, X. Rao, and B. Liu, “Weak magnetism stress internal testing technology of the long distance oil-gas pipeline,” *Journal of Mechanical Engineering*, vol. 53, no. 12, pp. 19–27, 2017.
- [21] Y. F. Duan, R. Zhang, Y. Zhao, S.-W. Or, K.-Q. Fan, and Z.-F. Tang, “Smart-Elasto-Magneto-Electric (EME) sensors for stress monitoring of steel structures in railway infrastructures,” *Journal of Zhejiang University Science A*, vol. 12, no. 12, pp. 895–901, 2012.
- [22] H. Zhang, Z. Tian, and Y. Duan, “Elasto-magnetic effect based suspender force monitoring of an arch bridge,” *Structural Engineers*, vol. 32, no. 4, pp. 80–84, 2016.
- [23] J. Tenkamp, M. Haack, F. Walther, M. Weibring, and P. Tenberge, “Application of micro-magnetic testing systems for non-destructive analysis of wear progress in casehardened 16MnCr5 gear wheels,” *Materialprüfung/Materials Testing*, vol. 58, no. 9, pp. 709–716, 2016.
- [24] W. Zhu, H. Qin, J. Li, and J. Ou, “Monitoring cable force of FAST project based on fiber bragg grating sensor external installed on anchorage zone,” *Journal of Mechanical Engineering*, vol. 53, no. 17, pp. 23–30, 2017.
- [25] X. Liu, B. Wang, Y. Ren, and Q. Huang, “Temporal and spatial evaluation method of monitoring cable forces for cable-stayed bridge,” *Journal of Harbin Institute of Technology*, vol. 50, no. 9, pp. 36–39, 2018.
- [26] S. M. Kolokolnikov, A. A. Dubov, and A. Y. Marchenkov, “Determination of mechanical properties of metal of welded joints by strength parameters in the stress concentration zones detected by the metal magnetic memory method,” *Welding in the World*, vol. 58, no. 5, pp. 699–706, 2014.
- [27] C. Li, L. Dong, and H. Wang, “Current research and development prospects of magnetic non-destructive assessment techniques for fatigue damage,” *Material Guide A: Summary*, vol. 29, no. 6, pp. 107–113, 2015.
- [28] S. G. Sandomirsky, “Analysis of the error in measuring the magnetic permeability of a ferromagnetic material in an open magnetic circuit,” *Measurement Techniques*, vol. 53, no. 9, pp. 1060–1066, 2010.
- [29] G. Weng, Y. Min, and B. Dai, “Magnetic coupling effect and on-line nondestructive stress detection of pipeline steel,” *Journal of Xi’an Shiyou University (Natural Science Edition)*, vol. 34, no. 5, pp. 104–109, 2019.